The Formation of a "Ghost" Electron Beam Via Electron-Ion Trapping at the Gun Test Stand

Joshua Yoskowitz

February 27, 2019

Introduction and Motivation

- Ions generally have negative effects on performance of electron accelerators and stability of electron beams
  - Quantum efficiency (QE) degradation of the photocathode due to ion back-bombardment [1,2]
  - Fast Ion Instability - ions that last for only one pass of a linac or storage ring (i.e. fast ions) can cause instabilities in the electron beam [3,4]
  - Charge neutralization due to trapped ions within an electron beam, causing beam loss [5]
- Mitigation techniques exist to reduce the effects of ions and clear them from the accelerator:
  - Clearing Electrodes - ions are attracted to the electrode and leave the electron beam [6]
  - Bunch Gaps - trapped ions leave the electron beam within bunch gaps introduced in the electron beam [7]
- Few (if any) techniques exist to directly measure and characterize ion production within an accelerator.

Discovery and Creation of Ghost Beam

- After running an electron beam at the Gun Test Stand for several minutes with the gun solenoid and biased anode on, a low intensity electron beam, measureable on a viewer downstream of the photocathode, still exists and is long lasting!
  - We know that this low intensity beam is made up of electrons due to how the beam steers with corrector magnets along the beam line.

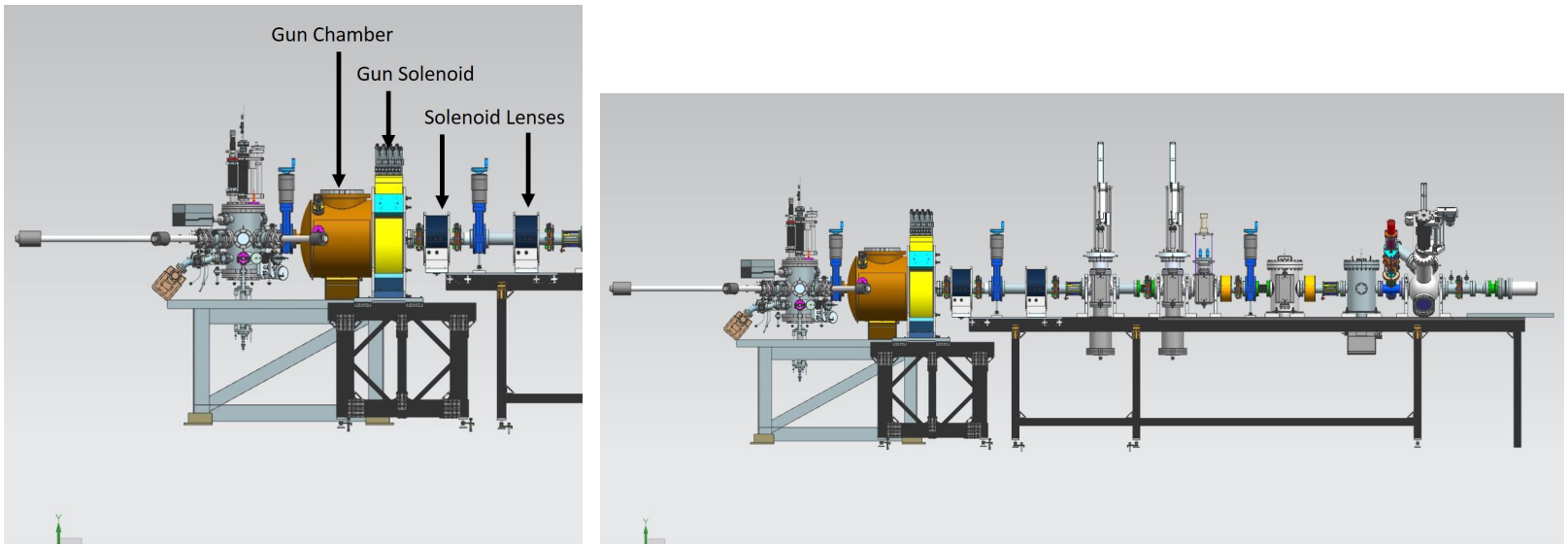

Figure: Diagrams of the GTS beamline

Discovery and Creation of Ghost Beam

- Current theory as to why this "ghost beam" exists:
  1. Real electron beam ionizes residual gas, creating ions and secondary electrons
  2. After the electron beam is turned off, these ions and secondary electrons remain trapped within the solenoid lenses via the magnetic mirror effect
  3. Ions and secondary electrons recombine and emit light, referred to here as "ghost light"
  4. Some of the ghost light hits the photocathode and creates electrons that are incident on the viewer
- Measuring the ghost light may be a way to measure and characterize ion production within the accelerator.

Process 1: Ionization of Residual Gas

- When residual gas molecules in the accelerator come into contact with the electron beam, the electrons can ionize the gas molecules, turning them into positive ions.
- The ion production rate depends upon the densities of the residual gas n_g, the density of the electron beam n_e, the ionization cross section σ_g, and the relative velocity of the electron beam $\beta_e c$

$$\frac{dn_i}{dt} = n_g n_e \sigma_g \beta_e c$$

- Note that n_i is the ion *density*. We can make this equation more meaningful by solving for the ion production rate per unit length.

$$\frac{d}{dt}\left(\frac{N_i}{l}\right) = n_g \sigma_g \frac{I_e}{e} = \frac{P_g \sigma_g}{k_B T_g}\frac{I_e}{e}$$

- The ionization cross section σ_g is derived from Bethe's theory[8,9]:

$$\sigma_g(\beta_e) = \frac{8a_0^2 \pi I_R A_1}{m_e c^2 \beta_e^2} f(\beta_e)\left(\ln\frac{2A_2 m_e c^2 \beta_e^2 \gamma^2}{I_R} - \beta_e^2\right)$$

$$= \frac{1.872 \times 10^{-24} A_1}{\beta_e^2} f(\beta_e)\left[\ln\left(7.515 \times 10^4 A_2 \beta_e^2 \gamma^2\right) - \beta_e^2\right]$$

$$f(\beta_e) = \frac{I_i}{T_e}\left(\frac{T_e}{I_i} - 1\right) = \frac{2I_i}{m_e c^2 \beta_e^2}\left(\frac{m_e c^2 \beta_e^2}{2I_i} - 1\right)$$

Process 1: Ionization of Residual Gas cont'd

- Below are log-log plots of ionization cross section σ_g vs. beam energy T_e and ion production rate per unit length $\frac{d}{dt}\left(\frac{N_i}{l}\right)$ vs. beam current I_e for 100keV electrons ionizing H_2 gas.

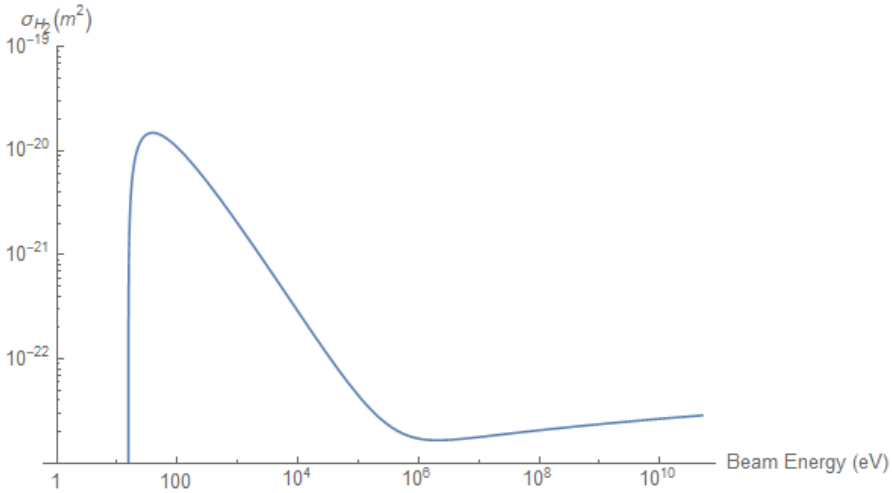

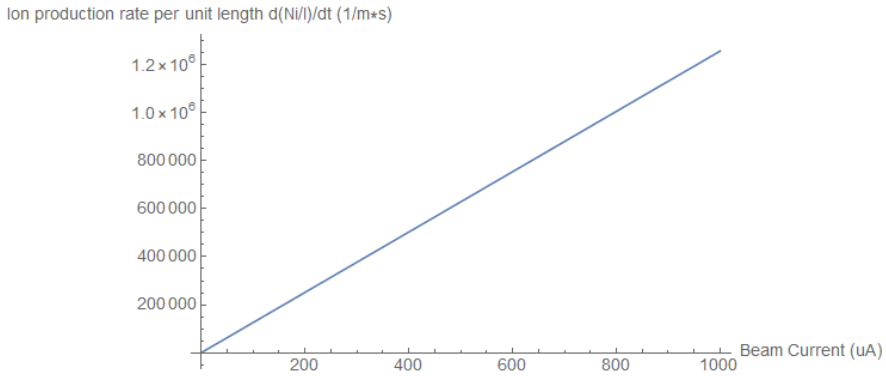

Process 1: Plugging in Numbers

- Assume that the residual gas is made up of only H_2 gas
- Plugging in numbers from 11/20/18 run:
  - $I = 100\mu A$
  - $T_e = 100keV$, $\beta_e c = 0.548c$
  - $P_g = 1.8 \times 10^{-8} Pa = 1.3 \times 10^{-10} torr$
  - $T_g = 293.15K$ (Room temperature)
- $\boxed{\sigma_{H_2} = 4.49 \times 10^{-23} m^2}$ and $\boxed{\frac{d}{dt}\left(\frac{N_{H_2^+}}{I}\right) = 1.25 \times 10^5 \ H_2^+ / (m \times s)}$

Process 1a: Secondary Electron Production

- When residual gas molecules are ionized by electrons, an electron is released from the molecule, as shown in the diagram below. This ejected electron is called a secondary electron.
- The secondary electron has much less kinetic energy than the primary (scattered) electron.
- We can determine the energy distribution of secondary electrons based on the differential cross section [10]:

$$\frac{d\sigma}{dW} = \iint \frac{d^3\sigma}{dW d\Omega_s d\Omega_p} d\Omega_s d\Omega_p$$

where W is the secondary electron energy and Ω_s and Ω_p are the solid angles of the secondary and primary electrons respectively.

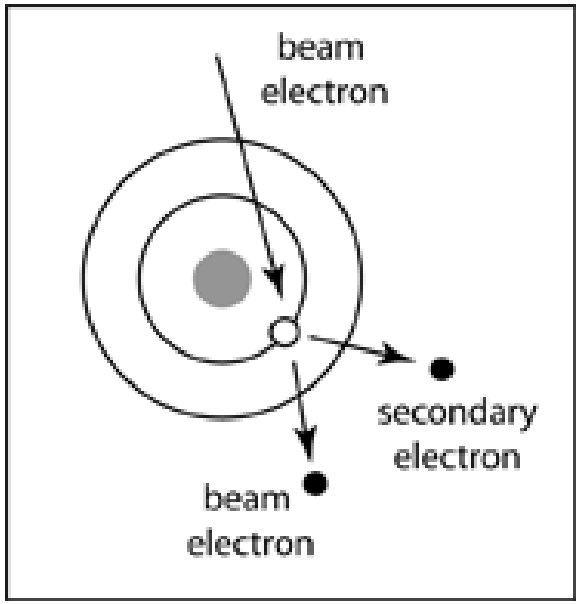

Process 1a: Secondary Electron Production cont'd

- Define the energy ratios t, w, and u as

$$t = \frac{T}{B}$$
$$w = \frac{W}{B}$$
$$u = \frac{U}{B}$$

where T is the incident electron energy, B is the binding energy, and $U = \langle p^2 \rangle / 2m$ is the average kinetic energy of the electrons in the subshell (from which the secondary electron was ejected). Note that $T \geq B + W$.

- Using these ratios, we can write the SDCS in the Binary Encounter Dipole model as [10,11]

$$\frac{d\sigma}{dW}(T, W) = \frac{4\pi a_0^2 R^2 N}{B^3 (t + u + 1)} \left[\frac{(N_i/N) - 2}{t + 1} \left(\frac{1}{w + 1} + \frac{1}{t - w} \right) + \left(2 - \frac{N_i}{N} \right) \left[\frac{1}{(w + 1)^2} + \frac{1}{(t - w)^2} \right] + \frac{\ln t}{N (w + 1)} \frac{df}{dw} \right]$$

$$N_i \equiv \int_0^\infty \frac{df(w)}{dw} dw$$

where a_0 is the Bohr radius, R is the Rydberg energy and N is the number of orbital electrons. Values for B, U, N, and $\frac{df}{dw}$ for H_2 are listed here [11].

Process 1a: Secondary Electron Production cont'd

- For a 100keV electron beam, we can plot the differential cross section $\frac{d\sigma}{dW}$ as a function of the secondary electron energy W.

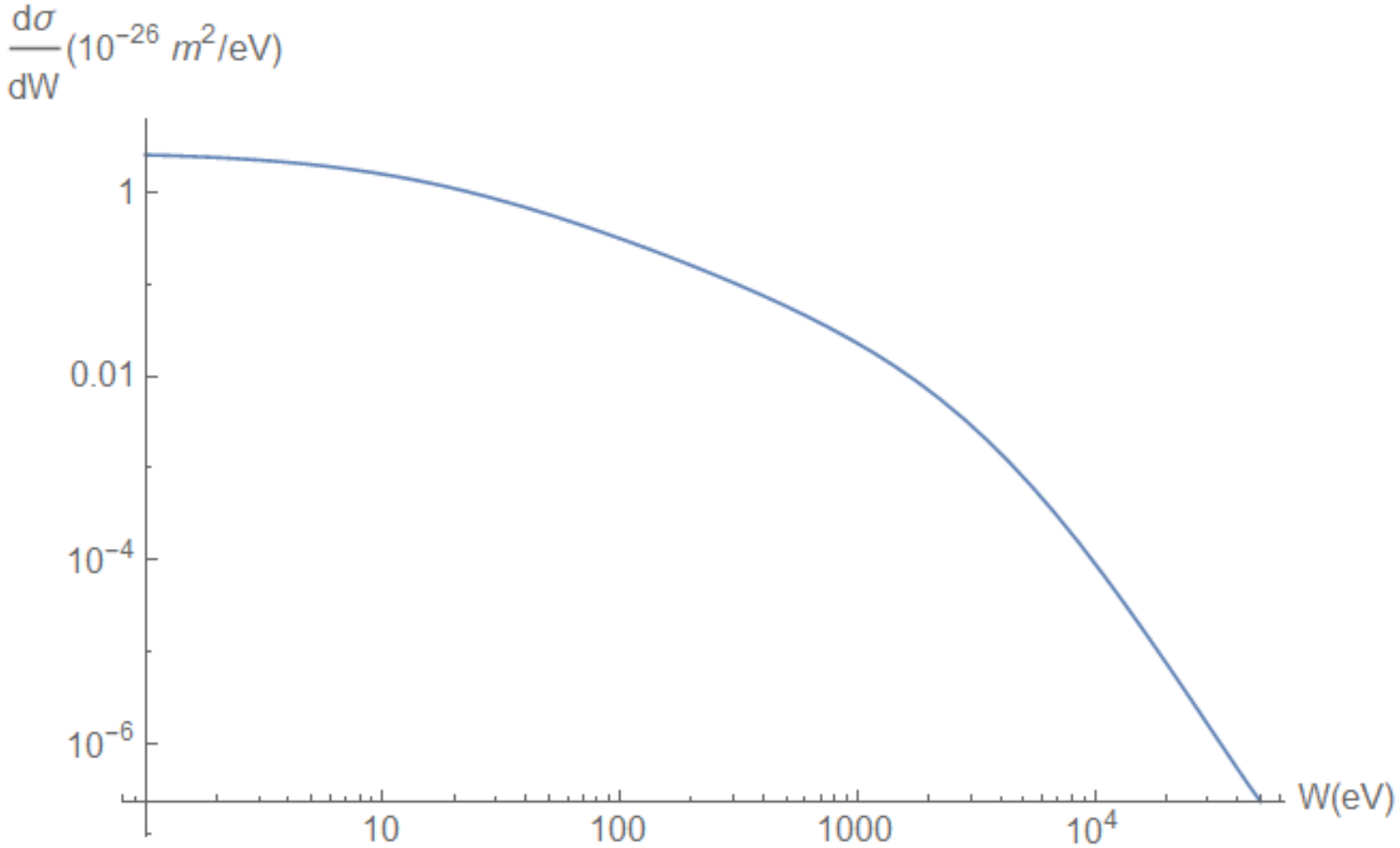

Process 2: Electron-Ion Trapping via Magnetic Mirror Effect

- Under certain conditions, charged particles and molecules can be trapped between two magnetic fields that have high gradient (between two strong solenoids, e.g.) via the magnetic mirror effect.
- Below is a plot of the z-component of magnetic field experienced by charged particles in the GTS beamline due to B-fields from the gun solenoid and two focusing solenoids. From the 11/20/18 run, the current in the gun solenoid is at 150A and the current in the two solenoids lenses are ~ 0.75A.

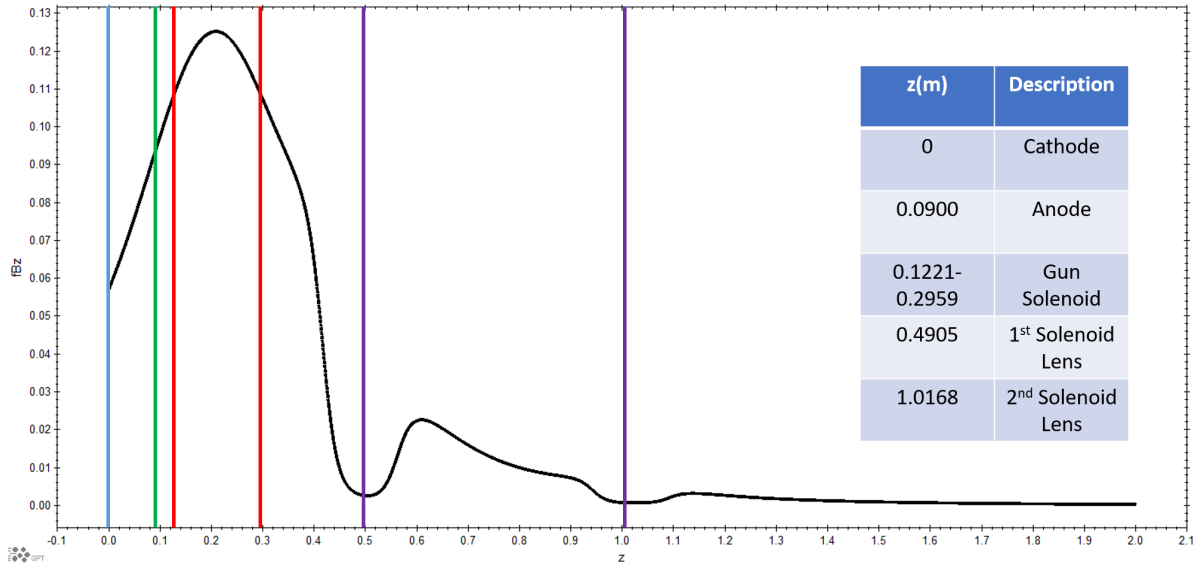

Process 2: Electron-Ion Trapping via Magnetic Mirror Effect cont'd

- Charged particles in the presence of a uniform longitudinal magnetic field B that is axially symmetric will circulate about the central axis at the Larmor radius:

$$r_L = \frac{mv_\perp}{qB}$$

where m and q are the mass and charge of the particle and $v_\perp$ is its orbital velocity.

- The magnetic moment μ of the particle is

$$\mu = \frac{1}{2}\frac{mv_\perp^2}{B}$$

which is a constant of the motion.[12]

- From energy conservation:

$$\frac{dE}{dt} = \frac{d}{dt}\left(\frac{1}{2}mv_\perp^2 + \frac{1}{2}mv_\parallel^2\right) = 0$$

- Thus, if a charged particle in a magnetic fields moves towards a higher magnetic field, then $v_\perp$ increases and $v_\parallel$ decreases. If the magnetic field is sufficiently strong, the particle will mirror.

Process 2: Electron-Ion Trapping via Magnetic Mirror Effect cont'd

- We can define a pitch angle, given by $\sin\theta = \frac{v_\perp}{v}$, above which the particle will always mirror. Using the invariance of μ, the threshold pitch angle θ is given by

$$\sin^2\theta_m = \frac{B_1}{B_2} \tag{1}$$

  where B_2 is the maximum B-field with $B_2 > B_1$ and $\theta \in [0°, 90°]$

- θ_m does not uniquely define the kinetic energy T of the particle. If we only consider particles that have Larmor radii within the radius of the beampipe ($r = 0.034$m), then we can define threshold pitch angles θ and kinetic energies T_{th}, given by

$$T_{th} = (\gamma_{th} - 1)\, mc^2$$

$$\gamma_{th} = \left(1 - \frac{v_{th}^2}{c^2}\right)^{-\frac{1}{2}}$$

$$v_{th} = \frac{v_{\perp,th}}{\theta_m}$$

  for electrons and for H_2^+ ions.

Process 2: Electron-Ion Trapping via Magnetic Mirror Effect cont'd

	Electrons/H_2^+ ions
Threshold θ for Lens 1, upstream ($B_{0.5} \rightarrow B_{0.21}$)	8.29°
Threshold θ for Lens 1, downstream ($B_{0.5} \rightarrow B_{0.61}$)	20.0°
Threshold θ for Lens 2, upstream ($B_{1.03} \rightarrow B_{0.9}$)	19.0°
Threshold θ for Lens 2, downstream ($B_{1.03} \rightarrow B_{1.13}$)	30.0°

	Electrons	H_2^+ ions
T_{th} for Lens 1, upstream ($B_{0.5} \rightarrow B_{0.21}$)	39.9keV	9.725eV
T_{th} for Lens 1, downstream ($B_{0.5} \rightarrow B_{0.61}$)	6.5keV	1.713eV
T_{th} for Lens 2, upstream ($B_{1.03} \rightarrow B_{0.9}$)	582eV	0.159eV
T_{th} for Lens 2, downstream ($B_{1.03} \rightarrow B_{1.13}$)	248eV	0.0675eV

Process 3: Electron-Ion Recombination

- When ions and electrons are brought together, there is a probability that the electron will recombine with the ion, resulting in a neutral atom/molecule and an emitted photon. This process is known as radiative recombination:

$$A^{Z+} + e^- \rightarrow A^{(Z-1)+}(n, l) + \gamma$$

The energy of the photon is $E_\gamma = E + E_{nl}$ where E is the incident electron energy and E_{nl} is the energy of an electron in the nl state of the target atom/molecule A.

- The total cross section for radiative recombination of an electron into state n is given by Pajek and Schuch and is based on Kramers formula[13]

$$\sigma_{tot}(E) = \frac{32\pi}{3\sqrt{3}}\alpha^3 a_0^2 \left(Z^2 E_0/E\right)\left[\gamma - s(n_{max}) + \ln\left(Z^2 E_0/E\right)^{1/2}\right]$$

where $\gamma \approx 0.577$ is the Euler constant (not to be confused with the photon γ) , α is the fine structure constant, E_0 is the Rydberg constant, a_0 is the Bohr radius, and $s(n_{max}) = \sum_{n=1}^{n_{max}} \frac{1 - g(n)}{n}$, where $n_{max} = 2$ for H_2 and values of $g(n)$ are given here[13].

Process 3: Electron-Ion Recombination cont'd

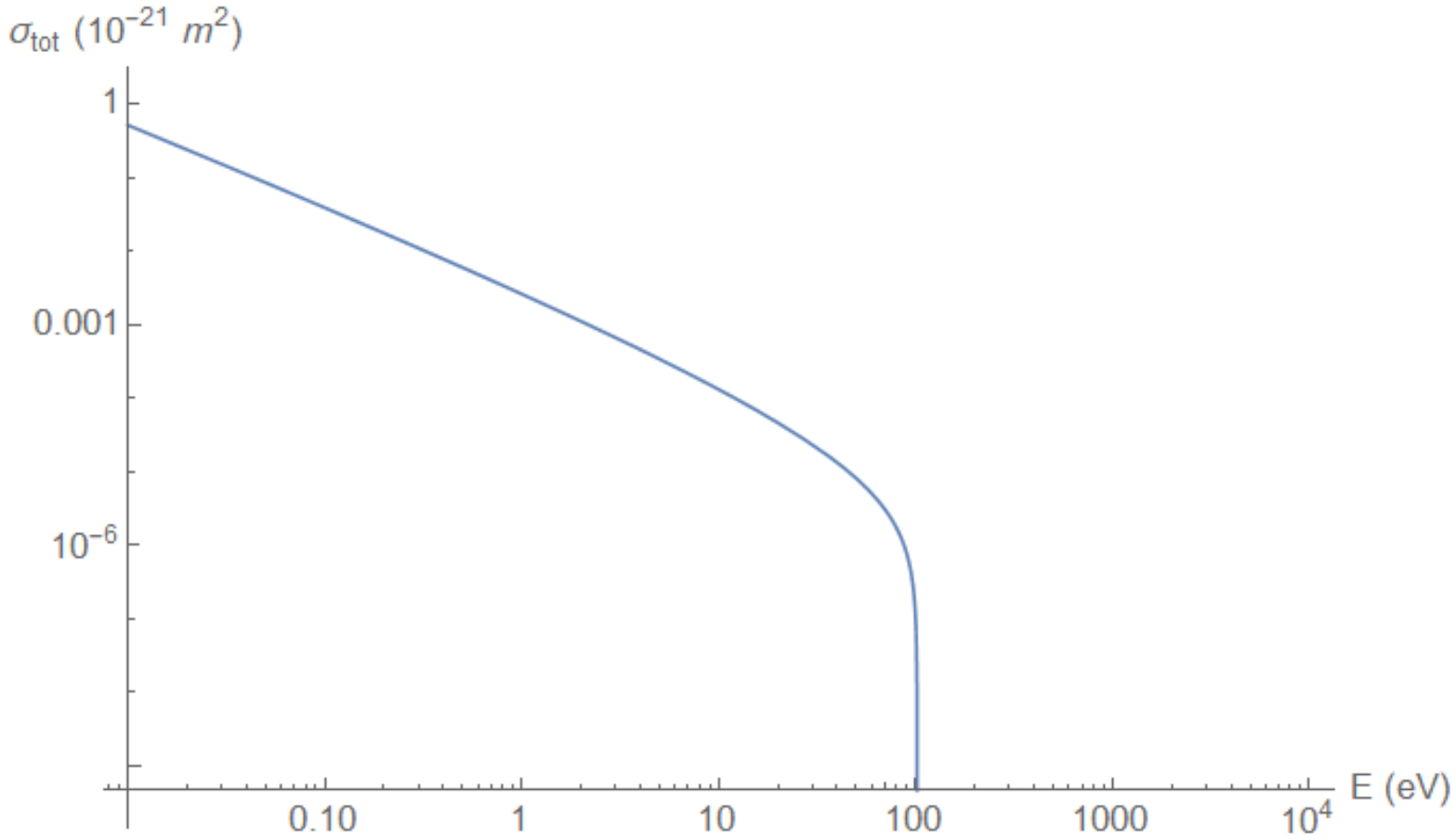

Figure: Log-log plot of $\sigma_{tot}(E)$ as a function of E for recombination with H_2^+ ions

Process 3: Electron-Ion Recombination cont'd

- The recombination rate α_{tot} is defined as the average of the product of $\sigma_{tot}(E)$ multiplied by the relative electron velocity for a given electron velocity distribution f:

$$\alpha_{tot} = \int v\sigma_{tot}(v) f(\vec{v}) d^3v$$

- Assuming a Maxwellian distribution, the recombination rate using $\sigma_{tot}(E)$ from Pajek and Schuch is given by[13]

$$\alpha_{tot} = \alpha_0 Z^2 \left(\frac{E_0}{kT_\perp}\right)^{\frac{1}{2}} \left[\frac{3}{2}\gamma - s(n_{max}) + \ln\left(Z^2 E_0/kT_\perp\right)^{1/2} + D(t)\right] G(t)$$

$$\alpha_0 = \left(\frac{32\pi}{3\sqrt{3}}\right)\alpha^3 a_0^2 \times 4\sqrt{\frac{E_0}{2\pi m_e}}$$

$$G(t) = \sqrt{\frac{t+1}{t}}\arctan\left(\sqrt{t}\right)$$

$$D(t) = \frac{1}{\arctan\sqrt{t}}\int_0^{\sqrt{t}} \frac{\ln\left(1+z^2\right)}{1+z^2} dz$$

$$t = \frac{kT_\perp - kT_\parallel}{kT_\parallel}$$

Note that this assumes that the recombining electron energy is much smaller than the binding energy (i.e. $E \ll E_{nl}$). In the case of H_2 and considering the graph of SDCS for $T_e = 100$keV, this assumption is valid.

Process 3: Electron-Ion Recombination cont'd

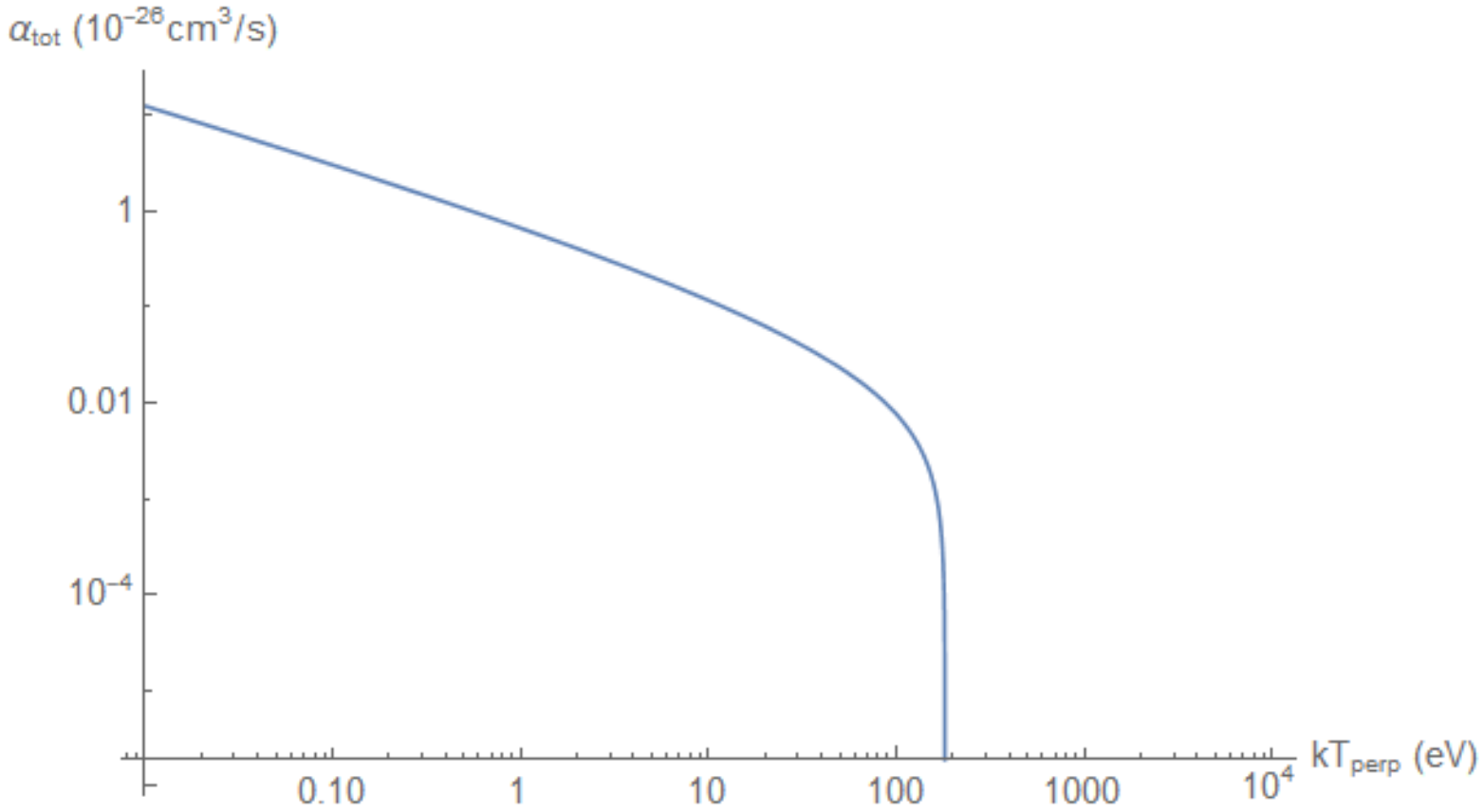

Figure: Log-log plot of α_{tot} vs. $kT_{\perp}$ for electrons recombining with H_2^+ ions.

Discussion

- In order to determine the average lifetime of a ghost beam, one must integrate all of these processes and iterate over all possible reaction channels. However, since there are so many possible reaction channels to ionization and recombination and because these processes are correlated, it is impractical to do this analytically.
- Instead, we can use simulation software such as GPT and IBSimu to simulate ionization, secondary electron production, and recombination. We can then record the lifetime of these processes and see if it matches the lifetimes measured in experiments.

Future Experiment and Connection to Thesis

- Two viewports will be added to the beamline within the gun solenoid.
  - The angled viewport will look for light emission between the anode and gun solenoid.
  - The perpendicular viewport will look for light emission in an artificial trap created by surrounding the viewport with steel shielding (like the solenoid lenses)
- If we measure ghost light, it would indicate that ions do exist in the accelerator and we can measure their concentrations and determine their identities.

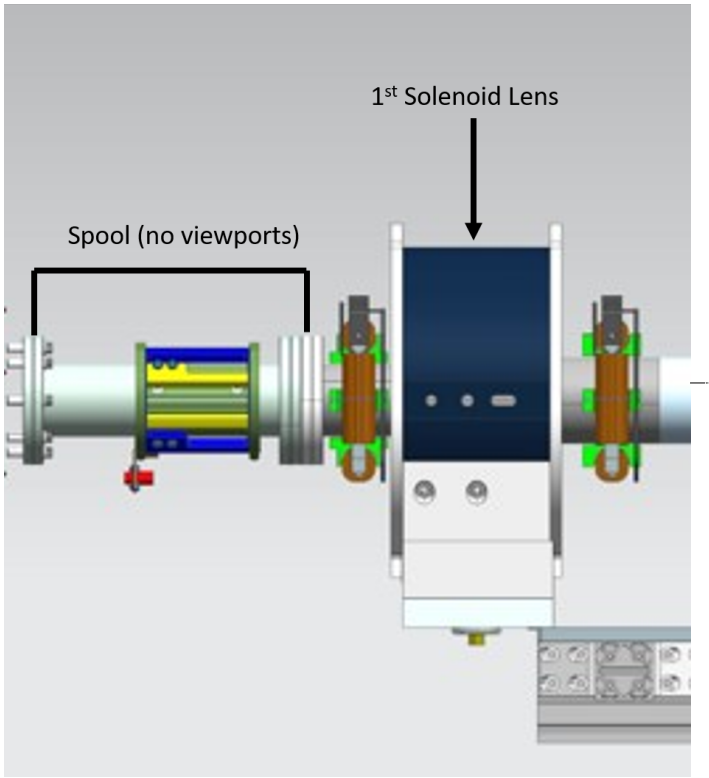

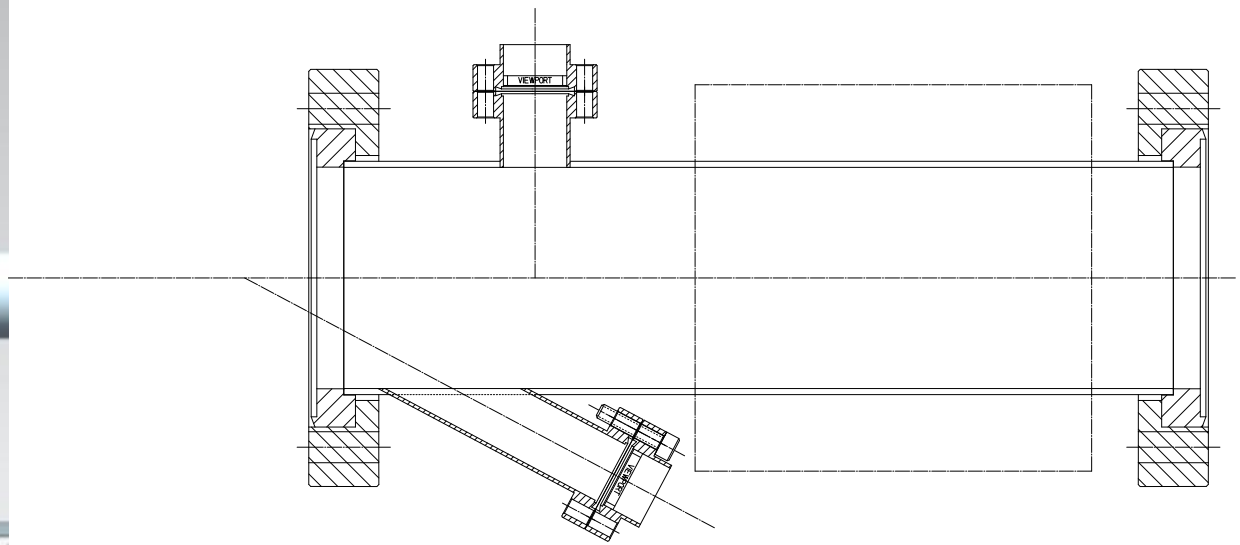

References

[1] J. Grames, P. Adderley, J. Brittian, D. Charles, J. Clark, J. Hansknecht, M. Poelker, M. Stutzman, and K. Surles-Law. Ion back bombardment of GaAs photocathodes inside dc high voltage electron guns. In *Proceedings of the 2005 Particle Accelerator Conference*, pages 2875–2877, May 2005. doi: 10.1109/PAC.2005.1591299.

[2] J. Grames, P. Adderley, J. Brittian, J. Clark, J. Hansknecht, D. Machie, M. Poelker, E. Pozdeyev, M. Stutzman, and K. Surles-Law. A biased anode to suppress ion back-bombardment in a dc high voltage photoelectron gun. *AIP Conference Proceedings*, 980(1):110–117, 2008. doi: 10.1063/1.2888075.

[3] Alex W. Chao. Lecture notes on topics in accelerator physics. Technical report, nov 2002.

[4] Avishek Chatterjee, Kelvin Blaser, Michael Ehrlichman, David Rubin, and James Shanks. Fast ion instability at cesr-ta. *Proceedings of the 5th Int. Particle Accelerator Conf.*, IPAC2014:Germany–, 2014. doi: 10.18429/jacow-ipac2014-tupri036.

[5] Yves Baconnier. Neutralization of accelerator beams by ionization of the residual gas, 1985.

[6] Steven Full, Adam Bartnik, Ivan Bazarov, John Dobbins, Bruce Dunham, and Georg Hoffstaetter. Detection and clearing of trapped ions in the high current cornell photoinjector. August 2015. doi: 10.1103/PhysRevAccelBeams.19.034201.

[7] Gisela Pöplau, Ursula van Rienen, and Atoosa Meseck. Numerical studies of the behavior of ionized residual gas in an energy recovering linac. *Physical Review Special Topics - Accelerators and Beams*, 18(4), apr 2015. doi: 10.1103/physrevstab.18.044401.

[8] H. Bethe. Zur theorie des durchgangs schneller korpuskularstrahlen durch materie. *Annalen der Physik*, 397(3):325–400, 1930. doi: 10.1002/andp.19303970303.

[9] Martin Reiser. *Theory and Design of Charged Particle Beams*. Wiley VCH Verlag GmbH, 2008. ISBN 3527407413.

[10] Yong-Ki Kim and M. Eugene Rudd. Binary-encounter-dipole model for electron-impact ionization. *Physical Review A*, 50(5):3954–3967, nov 1994. doi: 10.1103/physreva.50.3954.

[11] Ratko Janev, editor. *Atomic and Molecular Processes in Fusion Edge Plasmas*. Springer US, 1 edition, 1995. ISBN 0-306-45043-7.

[12] Peter T. Gallager. Introduction to plasma physics: Magnetic mirroring. 2013.

[13] M. Pajek and R. Schuch. Total radiative recombination rates for ions interacting with electrons from an electron cooler. *Nuclear Instruments and Methods in Physics Research Section B: Beam Interactions with Materials and Atoms*, 93(3):241–248, aug 1994. doi: 10.1016/0168-583x(94)95469-0.